MASSACHUSETTS INSTITUTE OF TECHNOLOGY
AEROELASTIC AND STRUCTURES RESEARCH LABORATORY

Technical Report 123-2

December 1965

APPROXIMATE SOLUTIONS FOR COMPUTING HELICOPTER HARMONIC AIRLOADS

by
Michael P. Scully

Department of the Navy
Bureau of Naval Weapons
Contract NOw 64-0188-d

MASSACHUSETTS INSTITUTE OF TECHNOLOGY
AEROELASTIC AND STRUCTURES RESEARCH LABORATORY
TECHNICAL REPORT 123-2

APPROXIMATE SOLUTIONS FOR COMPUTING HELICOPTER HARMONIC AIRLOADS

by
Michael P. Scully

Department of the Navy
Bureau of Naval Weapons
Contract NOw 64-0188-d

ACKNOWLEDGEMENTS

Grateful acknowledgement is made to Professor R. H. Miller for his supervision and advice, to Mrs. Nancy Ghareeb for her able programming, and to the MIT Computation Center for making available the necessary computer time.

SUMMARY

Assuming a constant circulation, rigid, trailing wake and using a lift deficiency function to represent the unsteady aerodynamic effects, various methods of calculating the airloads on a helicopter rotor in steady, forward flight were developed for the purpose of achieving: (a) faster solution times for a given level of accuracy and (b) a more accurate representation of the lifting surface/vortex interaction for the case where the blade passes close to the vortex line generated by a previous blade. Since most of the solution time is required to calculate the induced velocities due to the trailing wake, various approximate methods of calculating the induced velocities due to a rigid, skewed helix were developed. Within the limits of accuracy available from the rigid wake model either the solution of Reference (2), which represents the skewed helix with a series of infinite straight lines placed tangent to the helix whenever the helix passes under a blade, or the finite straight line solution, which represents the helix with a series of straight line segments subtending equal $\Delta\phi$ (change in azimuth angle), using $\Delta\phi = 30^{\circ}$-40° were found to give the fastest results. If the model is refined to include, for example, a nonrigid wake, then the finite straight line solution with a $\Delta\phi$ of approximately 15° should be used. The use of a conventional two dimensional lifting surface theory was tried for the lifting surface/vortex interaction case and little improvement resulted. It is recommended that the use of more sophisticated lifting surface theories be investigated for this case.

TABLE OF CONTENTS

LIST OF FIGURES

LIST OF FIGURES
(cont'd)

SYMBOLS

A_n = coefficients of chordwise induced velocity distribution.

P = nondimensional induced velocity.

P_l = location of an element of vorticity in the trailing wake.

P_η = point on the blade at which induced velocity is calculated.

R = rotor radius.

TPP = tip path plane.

V = velocity perpendicular to blade in TPP.

W = $W^* / \left(\frac{\Gamma}{4\pi R}\right)$ nondimensional induced velocity due to a vortex segment.

W^* = induced velocity due to a vortex segment.

$\vec{W}$ = $W\vec{n}$.

$\vec{a}$, $\vec{b}$ = vectors from P_η to the ends of the vortex segment.

a_o = zeroth harmonic of flapping.

b = blade semichord.

$\vec{c}$ = $\vec{a} - \vec{b}$.

d = nondimensional distance travelled by the rotor hub between t_ℓ and t_η.

h = h^*/R.

h^* = perpendicular distance from P_η to the vortex segment.

$\vec{i}, \vec{j}, \vec{k}$ = unit vectors in x, y, z directions (see Figure 24).

ℓ = nondimensional radial distance from the rotor hub to P_ℓ (part A).

$\vec{n}$ = unit vector from P_η parallel to the induced velocity at P_η.

t_ℓ = instant at which the element of vorticity at P_ℓ was trailed.

t_η = instant at which the induced velocity at P_η is calculated.

$v(x)$ = chordwise induced velocity distribution.

x, x_1 = x - components of the distances from P_η to the ends of the vortex segment

x = chordwise coordinate (Section III).

y, y_1 = y-components of distances from P_η to the ends of the vortex segment.

z, z_1 = z-components of distances from P_η to the ends of the vortex segment.

Γ = circulation of trailing vortex (constant).

Ω = angular velocity of rotor, radians/sec.

α, β = angles between lines from P_η to the vortex segment and the vortex segment (see Figure 23).

$\gamma_\pm$ = angles between the tangent to the spiral and the two half-infinite vortices (see Figure 22).

δ = angle between the induced velocity vector and the perpendicular to the TPP.

ς = angle between the blade which trailed the element of vorticity and the blade on which induced velocity

is being calculated, at any instant.

η = nondimensional radial distance from rotor hub to P_η .

θ = angle in the TPP between the local wind and the perpendicular to the blade at point P_η .

λ = nondimensional mean inflow.

$\lambda_{nc}, \lambda_{ns}$ = nondimensional $n^{'th}$ harmonics of inflow.

μ = advance ratio (tip speed ratio).

ν = $\phi - \psi - \theta$ (see Figure 14).

$\nu_\pm$ = See Figure 16.

ϕ = azimuth angle of blade trailing the element of vorticity at point P_ℓ at the instant of trailing (time t_ℓ).

$\Delta\phi$ = change in azimuth angle between the ends of a vortex segment.

$\delta\phi$ = change in azimuth angle between the nearest point and the other intersection of the half-infinite vortex and the spiral (see Figure 16).

ψ = azimuth angle of the blade upon which P_η is located at time t_η .

BLANK PAGE

I. INTRODUCTION

This report discusses various methods for computing blade airloads which were developed for the purpose of achieving: (a) faster solution times and (b) a more accurate representation of the lifting surface/vortex interaction for the case where the blade passes close to the vortex line generated by a previous blade.

The original solution for the induced velocity in forward flight due to the trailing wake used numerical integration down the spiral wake (Reference 1). This method required small interval sizes (typically 7.5^{o} in azimuth) and, hence, large amounts of computer time to get accurate results. A solution was also developed (Reference 2) where the spiral wake is replaced by a set of infinite straight line vortices (for which the induced velocity is known) placed tangent to the spiral at every point where the spiral passes under a blade during the first turn of the spiral. This solution is 20 times as fast as the numerical integration solution; however, it is less accurate. Attempts were then made to develop approximate solutions which would be faster than the numerical integration solution and more accurate than the approximate solution outlined above. Two such attempts are described below.

Nearest Point

Instead of replacing the spiral trailing wake by

infinite straight lines placed wherever the spiral passed under a blade, it was decided to locate the infinite straight lines wherever the distance from the point at which the induced velocity was being calculated to the spiral was a local minimum or maximum (nearest points). As a further refinement, a double infinite straight line solution was developed which used two half infinite straight line vortices, both starting at the nearest point and proceeding in nearly opposite directions to infinity, intersecting the spiral at points $\delta\phi$ away from the nearest point on both sides (see Figure 1). An approximate lifting surface theory was also developed based on the single infinite straight line geometry. Appendix A discusses these solutions in more detail. Since these solutions proved to be both slower and less accurate than the finite straight line solution discussed below, they were discarded.

Finite Straight Line (FSL)

This solution replaces the spiral vortex trailing wake with a series of straight line segments (see Figure 2). Originally, it was intended to take shorter line segments in the vicinity of nearest points and longer segments elsewhere. Due to the considerable amount of computer time involved in finding all the nearest points, however, a solution using a constant $\Delta\phi$ (change in azimuth angle) per line segment proved to be faster for equivalent accuracy.

Since FSL is approximately six times as fast as the

numerical integration method for equivalent accuracy, it has been adopted as the normal method of calculating induced velocities. It is even used for distorted wake cases where the trailing wake is not a perfect spiral (skewed helix) but some more general shape (Reference 3). Appendix B discusses FSL in more detail.

II. RESULTS AND CONCLUSIONS

Since the airloads on the H-34 rotor are available from NASA Flight Test data (Reference 4), the airloads for a test case ($\mu = .2$, $\lambda = .025$) have been calculated using induced velocities calculated by the various approximate methods outlined above. This gives a standard against which the various methods can be compared. The airload calculations use a two vortex (one at the tip and one at the midspan point) constant circulation trailing wake with the unsteady aerodynamic effects accounted for by the appropriate lift-deficiency function (Reference 2). Since the lower harmonics of airload can be calculated reasonably accurately by uniform inflow methods, the airloads have been plotted with 0^{th}, 1st, and 2nd harmonics extracted to emphasize the higher harmonics which uniform inflow methods cannot calculate accurately. Figure 3, 4, 5, and 6 show the airloads at the 95% spanpoint ($\eta = .95$) as calculated using the various approximate methods of calculating induced velocity outlined above compared with the NASA Flight Test data (Reference 4). For comparison the older infinite straight line (Reference 2) and numerical integration (Reference 1) methods are shown in Figures 7 and 8(a) respectively. From these figures, it can be seen that although the various methods do not agree completely with each other, there is little difference as far as the ability to predict the experimental data is concerned. The finite straight line case (Figure 6) is shown for an interval size ($\Delta\phi$) of 15^{o}. A case with $\Delta\phi = 7.5^{o}$ has been computed which gives essentially the same results, and,

hence, convergence to the case $\Delta\phi \rightarrow 0$ has occurred and Figure 6 results in the correct solution. Since Figure 6 does not show complete agreement with the test results, the two trailing vortex, constant circulation, rigid wake model used is inadequate, the ability of the finite straight line approximation to represent the model being better than the ability of the model to represent the actual case. Therefore, the model requires further refinement, for example, as has been done in Reference 3 which discusses initial efforts to improve the model by finding a better approximation to the wake geometry than the assumption of a rigid wake.

It is, therefore, concluded that:-

1) If the two vortex, constant circulation, rigid wake model is used, either the infinite straight line approximation of Reference 2 (which is fastest) or the finite straight line approximation with a large interval size ($\Delta\phi = 30^{\circ} - 40^{\circ}$) should be used since the other methods discussed above are all slower and yield no better agreement with the Flight Test data.

2) Future work should concentrate on developing the model to include refinements such as a non-rigid wake geometry and a varying strength trailing wake. For these cases with a refined model, the finite straight line aproximation with an interval size ($\Delta\phi$) of approximately 15° should be used.

III. TWO DIMENSIONAL LIFTING SURFACE THEORY

When a vortex line passes close to a rotor blade, as occurs on mostly lightly loaded rotors, the lifting line representation of the rotor blade becomes of questionable accuracy due to the rapid variations of induced velocities over the blade chord.

In the Appendix of Reference 1, a two-dimensional lifting surface theory is developed. The induced velocity is written as

$$w(X) = \frac{A_0}{2} + \sum_{n=1}^{\infty} \frac{A_n}{2} \cos n\theta$$

where $x = b \cos\theta$ is the chordwise coordinate. It is then shown that

$$L = \pi\rho b \left[\frac{1}{2} \frac{\partial}{\partial t}\left(A_0 - \frac{1}{2}A_2\right)b + \frac{\partial}{\partial t}\left(A_0 + \frac{1}{2}A_1\right)b + V\left(A_0 + \frac{1}{2}A_1\right) \right].$$

The A's can be calculated by calculating the induced velocity at a number of chordwise stations (typically 7) and doing a chordwise harmonic analysis. This process takes approximately 7 times as long as the equivalent lifting line procedure.

It was observed that lifting surface theory results

only differed significantly from lifting line results in the vicinity of sharp peaks in the airloads. A program was, therefore, developed which normally used lifting line theory. Whenever the value of the integrand more than doubled or halved in one integration interval ($\Delta\phi$) the program shifted to lifting surface theory and when the integrand no longer doubled or halved in one $\Delta\phi$ the program shifted back to lifting line theory. This program was written using the method of calculating induced velocities by numerically integrating over the wake which was developed in Reference 1.

Figure 3 shows the comparison of lifting line and lifting surface airloads with harmonics below the third eliminated compared with test data (Reference 4). This is for a rigid wake, 4-blade, μ = .2, λ = .025, and η =.95 case. There is some effect due to the lifting surface theory and a marginal improvement in agreement with the experimental data. It is not felt that this particular lifting surface theory is worth pursuing further. Instead, work is proceeding on more complete lifting surface theories (Reference 5).

APPENDIX A

NEAREST POINT

1. Finding Nearest Points

First it is necessary to find a set of local nearest points for a rigid wake. Consider a case where one wishes to calculate the induced velocity at time t_η and at point P_η due to vorticity trailed at time t_ℓ from the nearest point P_ℓ. Point P_η is at a radial distance ηR from the rotor hub on a blade with azimuth angle ψ at t_η, where R is the rotor radius. Point P_ℓ is at a radial distance ℓR from the hub on a blade with azimuth angle ϕ at t_ℓ. Let Σ be the angle between the η blade and the ℓ blade at any instant ($\Sigma = \psi - \phi$ when $t_\eta = t_\ell$). Then $t_\eta - t_\ell = \frac{1}{\Omega}(\psi + \Sigma - \phi)$ where Ω is the angular velocity of the rotor ($d\psi/dt$). Therefore, the distance travelled by the rotor hub in time $t_\eta - t_\ell$ is $dR = V(t_\eta - t_\ell)$, where V is the hub velocity. If $\mu = V/\Omega R$ = advance ratio: (see Figure 9)

$$d = \mu(\psi + \Sigma - \phi)$$

The condition for P_ℓ to be a nearest point (or farthest point) is that the line from P_η to P_ℓ (of length a) be perpendicular to the tangent to the spiral vortex at P_ℓ. Define Θ as the angle between the tangent to the spiral vortex at P_ℓ and a line perpendicular to the ℓ blade at P_ℓ. From Figure 9 it follows that:

$$\eta \sin \psi = \ell \sin \phi - a \sin (\phi - \theta) \qquad (A.1)$$

$$\eta \cos \psi - \ell \cos \phi - a \cos (\phi - \theta) = d = \mu (\psi + \zeta - \phi) \qquad (A.2)$$

To find θ it is assumed that the vortex is trailed parallel to the local velocity vector, which is composed of two components: a velocity $\ell \Omega R$ perpendicular to the blade due to the rotation of the blade and a velocity parallel to the hub motion $V = \mu \Omega R$ due to the hub motion.

From Figure 10 it can be seen that:

$$\tan \theta = \frac{-\mu \cos \phi}{\ell + \mu \sin \phi} \qquad (A.3)$$

This set of Eqs. (A.1), (A.2), and (A.3) can be combined into one equation:

$$\mu (\ell \sin \phi + \mu) (\psi + \zeta - \phi) - \eta \mu \cos \psi + \mu \ell \cos \phi + \ell \eta \sin (\psi - \phi) = 0 \qquad (A.4)$$

which can be solved for ϕ on a digital computer by a Newton-Raphson iteration. However, there are many solutions over the intervals of interest (e.g., $\phi = 0 \longrightarrow 4\pi$) and finding all the solutions in such an interval takes a considerable amount of time.

Having solved Eq. (A.4) for ϕ one can now solve Eq. (A.3) for θ and the Eq. (A.1) for a.

$$\theta = \tan^{-1}\left(\frac{-\mu\cos\phi}{\ell+\mu\sin\phi}\right)$$

$$a = \frac{\eta\sin\psi - \ell\sin\phi}{\sin(\phi-\theta)}$$

2. Single Infinite Vortex

a. Lifting Line

To calculate the downwash P the following equation from Appendix B may be used:

$$W = \frac{\cos\alpha + \cos\beta}{h}$$

For an infinite straight line vortex $\alpha = \beta = 0$. From Figure 11:

$$h^2 = Z^2 + a^2 \quad , \quad P = -W\cos\delta$$

$$\cos\delta = a/h, \qquad P = \frac{-2a}{Z^2 + a^2}$$

Where the downwash P is, the induced velocity component perpendicular to the tip path plane (TPP), and z, the nondimensional displacement of the vortex below the TPP, is given by (for a rigid wake):

$$z = \lambda (\psi + \varsigma - \phi)$$

For the near wake case the vortex line is only half-infinite, hence $\alpha = 0$ but $\beta \neq 0$. From Figure 12:

$$\beta = \pi/2 - \theta \quad , \; h = (\ell - \eta) \cos\theta$$

$$P = \frac{1 + \sin\theta}{(\ell - \eta) \cos\theta}$$

Note that z = 0 here, and hence P = W.

b. Lifting Surface

In the Appendix of Reference 1, a lifting surface theory is developed. The induced velocity is written as:

$$W = v(x) = \frac{A_o}{2} + \sum_{n=1}^{\infty} \frac{A_n}{2} \cos n\theta$$

where $x = b \cos\theta$ is the chordwise coordinate. It is then shown that:

$$L = \pi\rho b \left[\frac{1}{2} \frac{\partial}{\partial t} (A_o - \tfrac{1}{2} A_2) b + \frac{\partial}{\partial t} (A_o + \tfrac{1}{2} A_1) b + V(A_o + \tfrac{1}{2} A_1) \right].$$

If A_1, $\frac{\partial A_1}{\partial t}$ and A_2 are neglected compared to A_o and $\frac{\partial A_o}{\partial t}$ then:

$$L = \pi\rho b \left[\frac{3}{2} b \frac{\partial A_o}{\partial t} + V A_o \right]$$

Noting that $\Omega = \frac{d\psi}{dt}$ then:

$$\frac{\partial A_o}{\partial t} = \frac{\partial A_o}{\partial \psi} \frac{d\psi}{dt} = \Omega \frac{\partial A_o}{\partial t}$$

Also:

$$V = \eta \Omega R \cos\theta + \Omega R \sin\psi$$

Hence:

$$L = \pi\rho b \left[\frac{3}{2} b \Omega \frac{\partial A_o}{\partial \psi} + (\eta \Omega R \cos\theta + \Omega R \sin\psi) A_o \right].$$

Figure 13 shows the type of error involved in neglecting A_1, $\frac{\partial A_1}{\partial t}$ and A_2. This figure is the result of calculating the downwash at seven chordwise stations, performing a chordwise harmonic analysis on the result, and using the resulting coefficients to calculate L.

A_o is simply the average value of the downwash as a function of x at any ψ and η. Thus A_o can be found by integrating the downwash over the chord and dividing by the chord.

$$A_o = \frac{1}{2(b/R)} \int_{-b/2R}^{3b/2R} \frac{2\,a_1(x)\,dx}{z^2 + a_1^2(x)}$$

From Figure 14:

$$a_1(x) = -a + x \sin\nu$$

where: $$\nu = \phi - \psi - \theta$$

Since the chord is small relative to the rate of change of z, one can assume that z is constant over the chord. Substituting and integrating:

$$A_o = \frac{1}{2(b/R)\sin\nu} \ln\left(\frac{4z^2 + 4a^2 - 12a\left(\frac{b}{R}\right)\sin\nu + 9\left(\frac{b}{R}\right)^2 \sin^2\nu}{4z^2 + 4a^2 + 4a\left(\frac{b}{R}\right)\sin\nu + \left(\frac{b}{R}\right)^2 \sin^2\nu}\right)$$

Noting that: $\nu = \phi - \psi - \theta$, $\therefore \frac{\partial\nu}{\partial\psi} = -1$

$$\therefore \frac{\partial A_o}{\partial\psi} = \frac{\partial A_o}{\partial\nu}\frac{\partial\nu}{\partial\psi} = -\frac{\partial A_o}{\partial\nu}$$

$$\therefore \frac{\partial A_0}{\partial \psi} = \frac{\cos\nu}{2\left(\frac{b}{R}\right)\sin^2\nu} \ln\left(\frac{4z^2+4a^2-12a\left(\frac{b}{R}\right)\sin\nu+9\left(\frac{b}{R}\right)^2\sin^2\nu}{4z^2+4a^2+4a\left(\frac{b}{R}\right)\sin\nu+\left(\frac{b}{R}\right)^2\sin^2\nu}\right)$$

$$-\left(\frac{1}{2\left(\frac{b}{R}\right)\sin\nu\left(4z^2+4a^2-12a\left(\frac{b}{R}\right)\sin\nu+9\left(\frac{b}{R}\right)^2\sin^2\nu\right)}\right)$$

$$\left[\left(-12a\left(\frac{b}{R}\right)\cos\nu+18\left(\frac{b}{R}\right)^2\sin\nu\cos\nu\right)-\left(\frac{4z^2+4a^2-12a\left(\frac{b}{R}\right)\sin\nu+9\left(\frac{b}{R}\right)^2\sin^2\nu}{4z^2+4a^2+4a\left(\frac{b}{R}\right)\sin\nu+\left(\frac{b}{R}\right)^2\sin^2\nu}\right)\right.$$

$$\left.\cdot\left(2\left(\frac{b}{R}\right)^2\sin\nu\cos\nu+4a\left(\frac{b}{R}\right)\cos\nu\right)\right] .$$

For the near wake it is assumed that the vortex originates at the same chordwise coordinate x as the point where downwash is calculated. From Figure 15:

$$\alpha = 0 \ , \beta = \frac{\pi}{2} + \theta \ , \text{ and } \ a = -(\ell-\eta)\cos\theta \ .$$

Thus for the near wake case, use the far wake equation multiplied by $\frac{1-\sin\theta}{2}$ and with $a = -(\ell-\eta)\cos\theta$.

3. Double Infinite Vortex

For this case, the downwash (P) is calculated in two parts (P_+ and P_-), one for each vortex. From Figure 16:

$$\tan\nu_+ = \frac{\ell\sin(\phi-\delta\phi)-\ell\sin\phi}{\ell\cos(\phi-\delta\phi)+\mu\delta\phi-\ell\cos\phi} \ , \gamma_+ = \phi-\frac{\pi}{2}-\theta-\nu_+ \ ,$$

$$\tan\nu_- = \frac{\ell\sin\phi-\ell\sin(\phi+\delta\phi)}{\ell\cos\phi+\mu\delta\phi-\ell\cos(\phi+\delta\phi)} \ , \gamma_- = \frac{\pi}{2}+\theta+\nu_--\phi \ .$$

From Figure 16 it can be seen that $h = a \cos \gamma_{\pm}$ and

$$\alpha_+ = \pi - \phi - \nu_+ \,, \beta_+ = 0 \,, \alpha_- = 0 \,, \beta_- = \phi - \nu_-$$

$$\therefore P_+ = \frac{-a \cos\gamma_+ [1 - \cos(\phi - \nu_+)]}{z^2 + a^2 \cos^2 \gamma_+} \,, P_- = \frac{-a \cos\gamma_- [1 + \cos(\phi - \nu_-)}{z^2 + a^2 \cos^2 \gamma_-}$$

For far wake $P = P_+ + P_-$ and for near wake $P = P_+$.

APPENDIX B

THE INDUCED VELOCITY OF A VORTEX SEGMENT

To calculate induced velocities, use may be made at the following relationship for a straight line vortex segment, derived from the Biot Savart Law (Reference 6).

$$W^* = \frac{\Gamma}{4\pi h^*} (\cos\alpha + \cos\beta)$$

where W* is the dimensional induced velocity at point P_η, perpendicular to the plane determined by the vortex segment and point P_η, Γ is the dimensional circulation of the vortex segment, h* is the perpendicular distance from the vortex segment to point P_η, and α and β are the angles between lines drawn from the ends of the vortex segment to point P_η and the vortex segment (see Figure 17). Now define the nondimensional quantities:

$$W \equiv W^* / \left(\frac{\Gamma}{4\pi R}\right) \quad \text{and} \quad h \equiv h^* / R$$

where R is the dimensional rotor radius. Therefore:

$$W = \frac{\cos\alpha + \cos\beta}{h}$$

APPENDIX C
FINITE STRAIGHT LINE (FSL)

Consider calculating the induced velocity at point P_η and time t_η . Point P_η is on the quarter chord line and at a spanwise distance from the rotor hub ηR on the blade at azimuth angle ψ at time t_η . To calculate the induced velocity due to the entire wake, consider a general vortex element at point P_ℓ , which is inducing part of the total induced velocity at P_η . Let t_ℓ be the time at which the element of vorticity at P_ℓ was trailed. Then at time t_ℓ point P_ℓ was on the quarter chord line and at a spanwise distance from the rotor hub ℓR on the blade at azimuth angle ϕ . Let the azimuth angle between the blade on which P_η is located and the blade which trailed the element of vorticity at P_ℓ at any instant be Σ . Hence, in the time from t_ℓ until t_η the rotor hub will move a nondimensional distance $d = \mu(\psi + \Sigma - \phi)$, where $\mu = V/\Omega R$ is the advance ratio. Similarly, the vertical displacement, perpendicular to the tip path plane (TPP), of point P_ℓ relative to point P_η at time t_η will be, nondimensionally, $z = \lambda(\psi + \Sigma - \phi)$ where λ is the nondimensional mean inflow through the rotor.

Define a right-handed axis system with origin at P_η . The y-azis and $\vec{j}$ are parallel to and in the opposite direction from the line of rotor hub motion, and are in the TPP. The x-axis and $\vec{i}$ are perpendicular to the y-axis and are in the TPP. The z-axis and $\vec{k}$ are perpendicular to the TPP and point downward (Figure 24). Let $\vec{i}$, $\vec{j}$, and $\vec{k}$ be unit vectors.

For convenient calculation the spiral wake is now broken up into a series of straight line segments of equal $\Delta\phi$ (typically 15°), where $\Delta\phi$ refers to the difference in azimuth angle ϕ between the ends of the vortex segment. P_ℓ is defined to be at the end of the vortex segment nearest P_η along the spiral. Define the coordinates of the ends of a typical vortex segment to be (x, y, z) and (x_1, y_1, z_1) (Figure 18). From Figure 19 and recalling the values of z and d:

$$X = \ell \sin\phi - \eta \sin\psi \quad , \quad X_1 = \ell \sin(\phi - \Delta\phi) - \eta \sin\psi$$

$$Y = \ell\cos\phi - \ell\cos\psi + \mu(\psi + \zeta - \phi)$$

$$Y_1 = \ell\cos(\phi - \Delta\phi) - \ell\cos\psi + \mu(\psi + \zeta - \phi + \Delta\phi)$$

$$Z = \lambda(\psi + \zeta - \phi) - a_0(\ell - \eta) \quad , \quad Z_1 = \lambda(\psi + \zeta - \phi + \Delta\phi) - a_0(\ell - \eta)$$

where a_0 is the coning angle.

From Appendix B, the nondimensional induced velocity is:

$$W = \frac{\cos\alpha + \cos\beta}{h}$$

Define $\vec{a}$ and $\vec{b}$ as vectors from P_η to the ends of the vortex segment and $\vec{c} = \vec{a} - \vec{b}$, then from Figure 18:

$$\cos\alpha = \frac{(-\vec{a})\cdot(-\vec{c})}{|\vec{a}||\vec{c}|} \quad , \quad \cos\beta = \frac{(-\vec{b})\cdot\vec{c}}{|\vec{b}||\vec{c}|}$$

$$h = |\vec{a}|\sin\alpha = |\vec{a}|\,\frac{|(-\vec{c})\times(-\vec{a})|}{|\vec{a}||\vec{c}|}$$

Define $\vec{n}$ as the unit vector parallel to the induced velocity at P_η, then from Figure 18:

$$\vec{n} = \frac{\vec{a}\times\vec{b}}{|\vec{a}\times\vec{b}|}$$

The induced velocity vector is:

$$\vec{W} = W\vec{n} = \left[\frac{\dfrac{(-\vec{a})\cdot(-\vec{c})}{|\vec{a}|} + \dfrac{(-\vec{b})\cdot\vec{c}}{|\vec{b}|}}{|(-\vec{c})\times(-\vec{a})|}\right]\left(\frac{\vec{a}\times\vec{b}}{|\vec{a}\times\vec{b}|}\right) .$$

From Figure 18:

$$\vec{a} = x\vec{i} + y\vec{j} + z\vec{k} \quad , \quad \vec{b} = x_1\vec{i} + y_1\vec{j} + z_1\vec{k}$$

$$\vec{c} = (x-x_1)\vec{i} + (y-y_1)\vec{j} + (z-z_1)\vec{k} .$$

Substituting and reducing results in:

$$\vec{W} = \left[\frac{\dfrac{x_1^2+y_1^2+z_1^2-xx_1-yy_1-zz_1}{\sqrt{x_1^2+y_1^2+z_1^2}} + \dfrac{x^2+y^2+z^2-xx_1-yy_1-zz_1}{\sqrt{x^2+y^2+z^2}}}{(yz_1-y_1z)^2+(x_1z-xz_1)^2+(xy_1-x_1y)^2} \right]$$

$$\left[(yz_1-y_1z)\vec{i} + (x_1z-xz_1)\vec{j} + (xy_1-x_1y)\vec{k} \right]$$

which can easily be programmed for rapid computation on a digital computer.

Now the $\vec{W}$ for the various segments of wake must be summed over ϕ between some limits. The upper limit is the upper end of the spiral vortex at time t_η . After several turns of the spiral P_ℓ becomes so far away from P_η that it induces a negligible velocity at P_η and can be neglected. A typical lower limit is two turns of the spiral (720° in ϕ) below the upper limit. After summing over ϕ summing over ℓ (for two trailing vortices ℓ = 1.0, .5, typically) and Σ (for 4 blades $\Sigma = 0, \pi/2, \pi$, and $3\pi/2$) gives the nondimensional induced velocity at P_η due to a rigid trailing wake of constant circulation.

REFERENCES

1. R. H. Miller: Rotor Blade Harmonic Air Loading. AIAA Journal, Vol. 2, No. 7 (July, 1964).

2. R. H. Miller: Unsteady Airloads on Helicopter Rotor Blades. Fourth Cierva Memorial Lecture to the Royal Aeronautical Society, Vol. 68, No. 640 (April, 1964).

3. M.P. Scully: Basic Techniques for Studies of Helicopter Vortex Wake Geometry and Some Preliminary Results. MIT Aeroelastic and Structures Research Laboratory TR 123-1, (to be published).

4. Preliminary Data from Floyd L. Thompson, NASA, Langley, (May 24, 1961).

5. J. P. Jones: An Extended Lifting Line Theory for the Loads on a Rotor Blade in the Vincinity of a Vortex. MIT, Aeroelastic and Structures Research Laboratory TR 123-3 (to be published).

6. H. Glauert: Aerofoil and Airscrew Theory. Cambridge University Press.

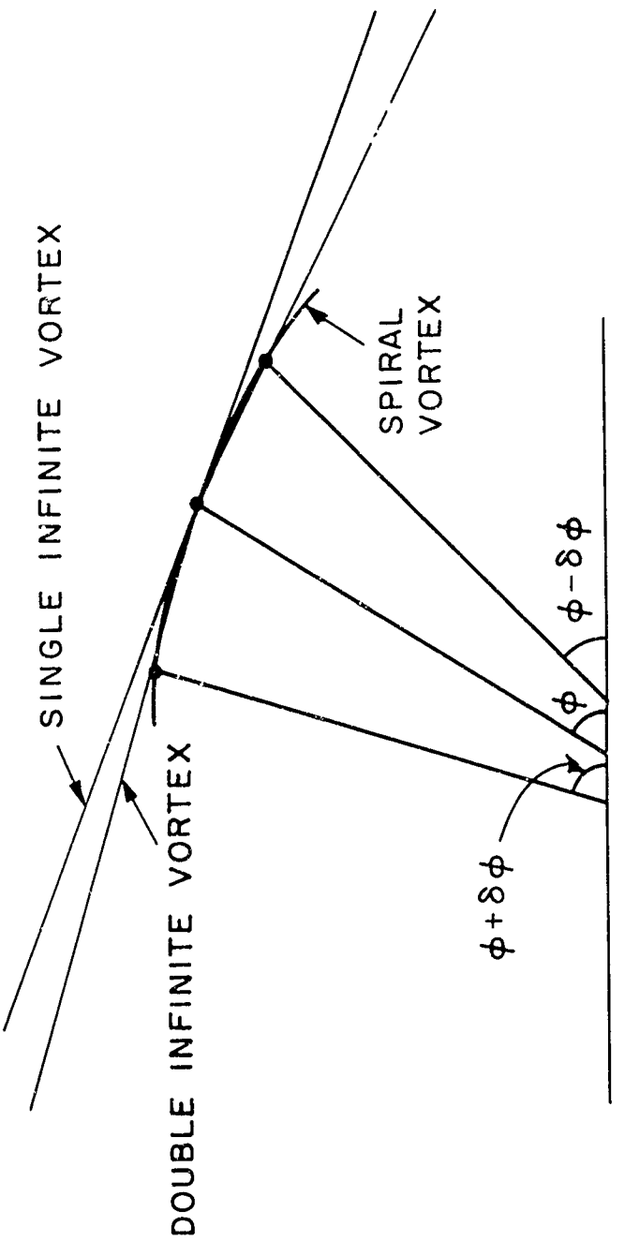

FIG.1 SINGLE AND DOUBLE INFINITE VORTEX APPROXIMATION

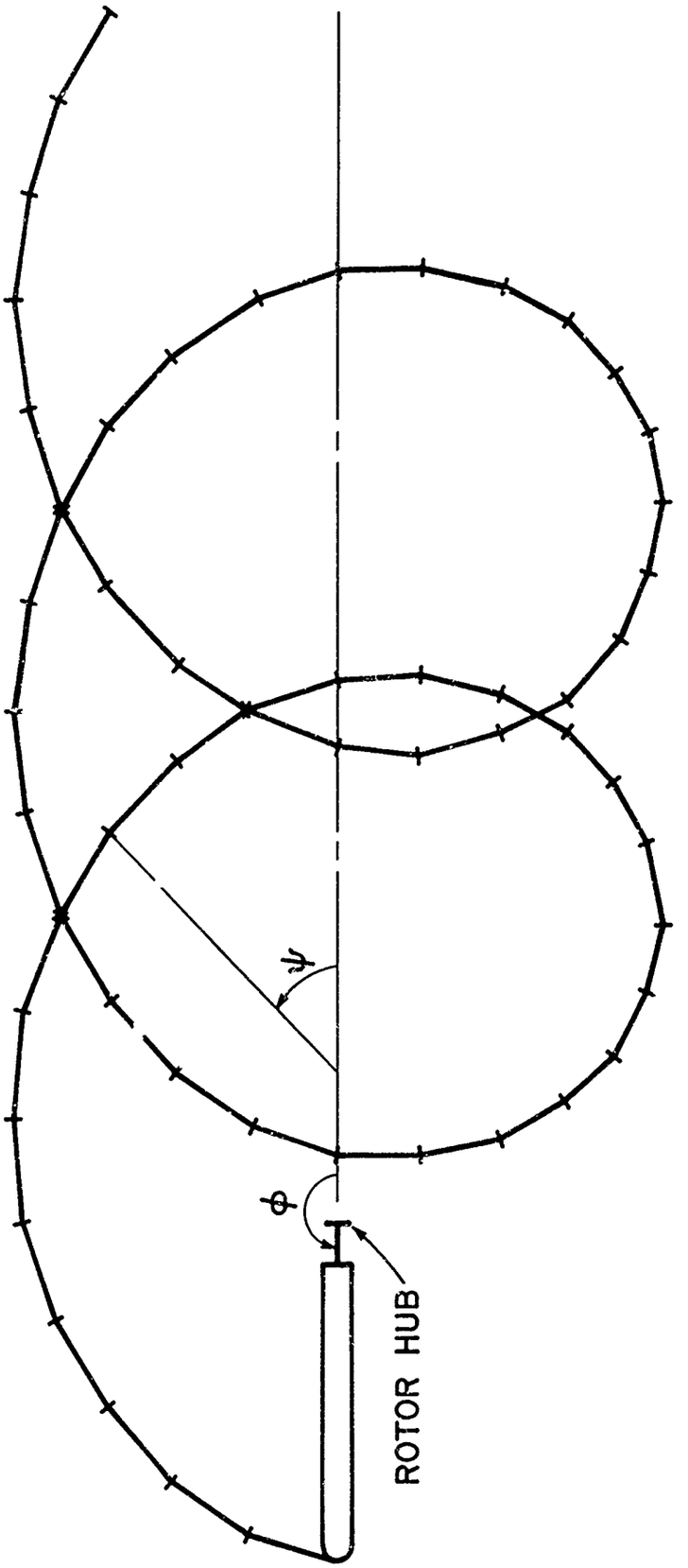

FIG. 2 FINITE STRAIGHT LINE APPROXIMATION

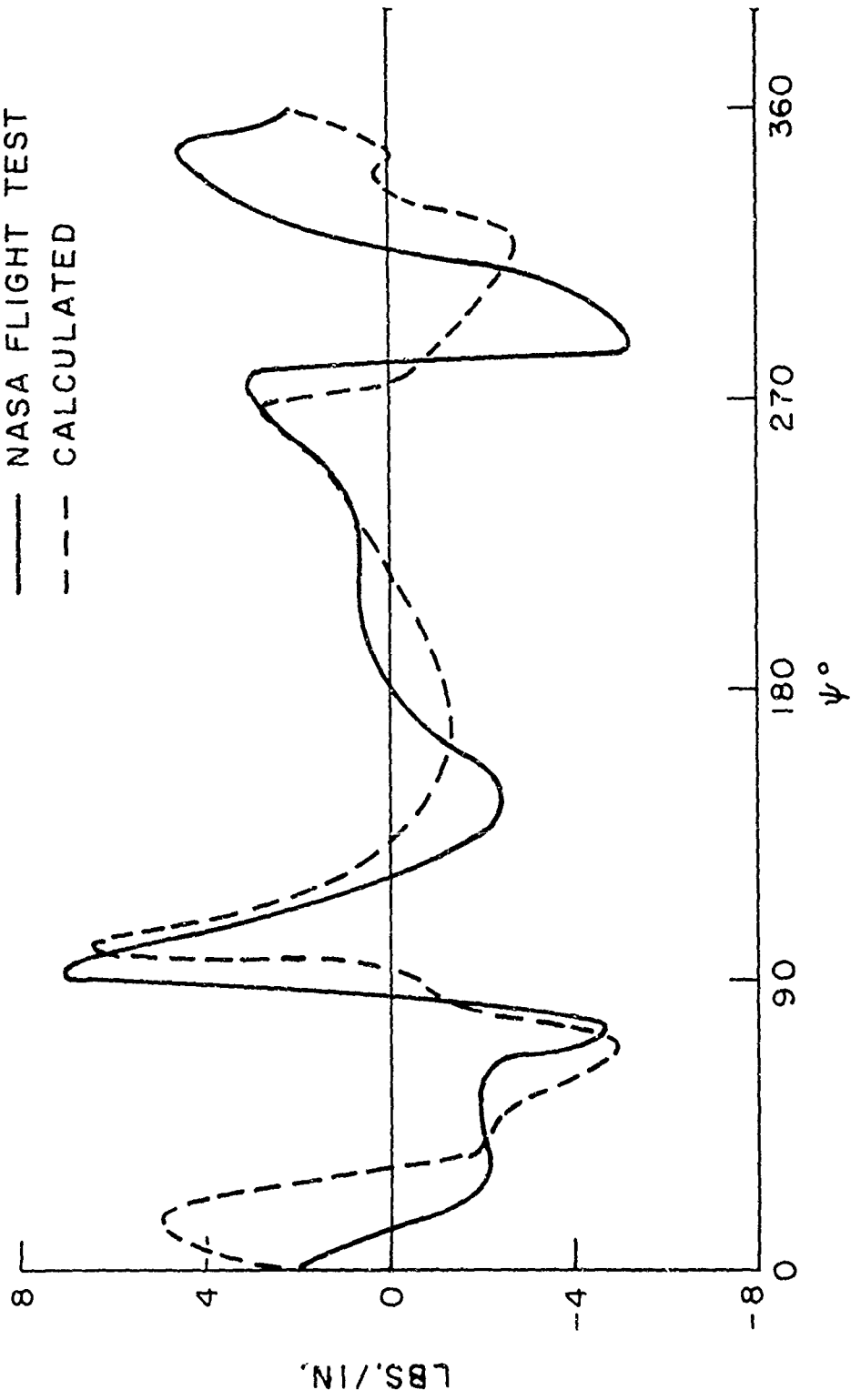

FIG. 3 AIRLOADS, 0th, 1st, AND 2nd HARMONICS EXTRACTED, NEAREST POINT – SINGLE INFINITE STRAIGHT LINE
4 BLADES, $\mu = 0.2$, $\lambda = 0.025$, $\eta = 0.95$

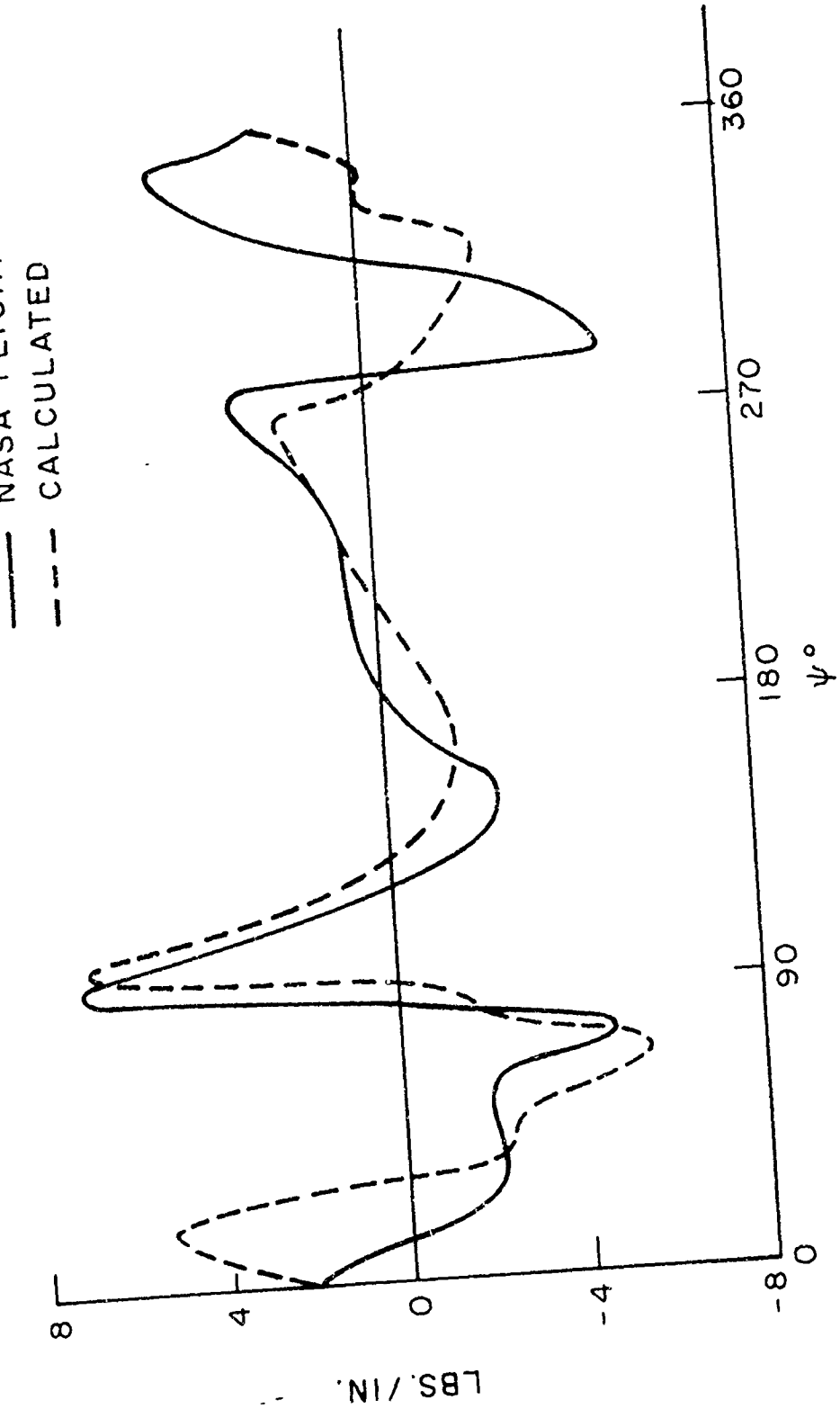

FIG. 4 AIRLOADS, 0th, 1st, AND 2nd HARMONICS EXTRACTED, NEAREST POINT-SINGLE INFINITE STRAIGHT LINE – LIFTING SURFACE.
4 BLADES, $\mu = 0.2$, $\lambda = 0.025$, $\eta = 0.95$

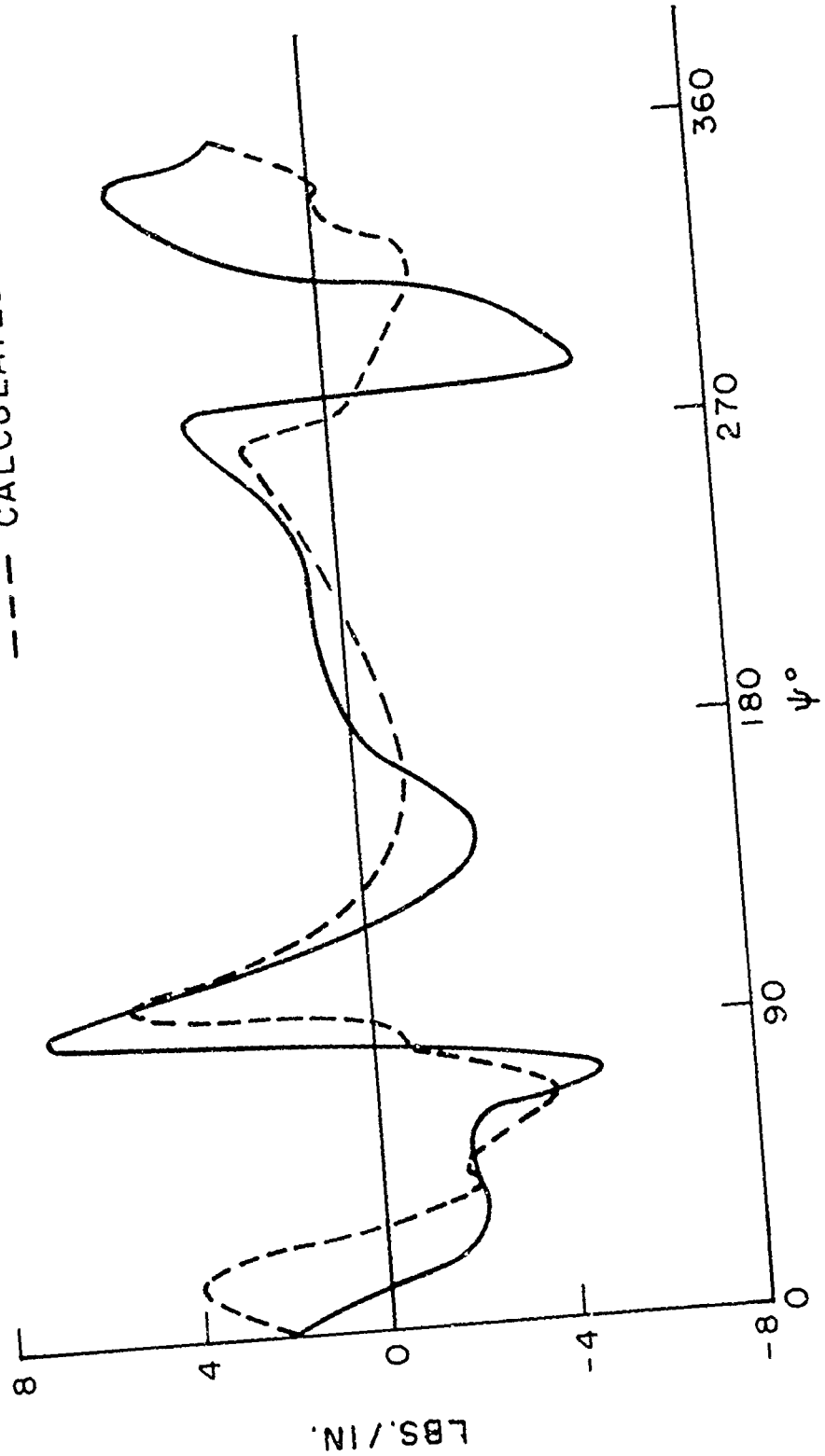

FIG. 5 AIRLOADS, 0th, 1st, AND 2nd HARMONICS EXTRACTED, NEAREST POINT - DOUBLE INFINITE STRAIGHT LINE. 4 BLADES, $\mu = 0.2$, $\lambda = 0.025$, $\eta = 0.95$

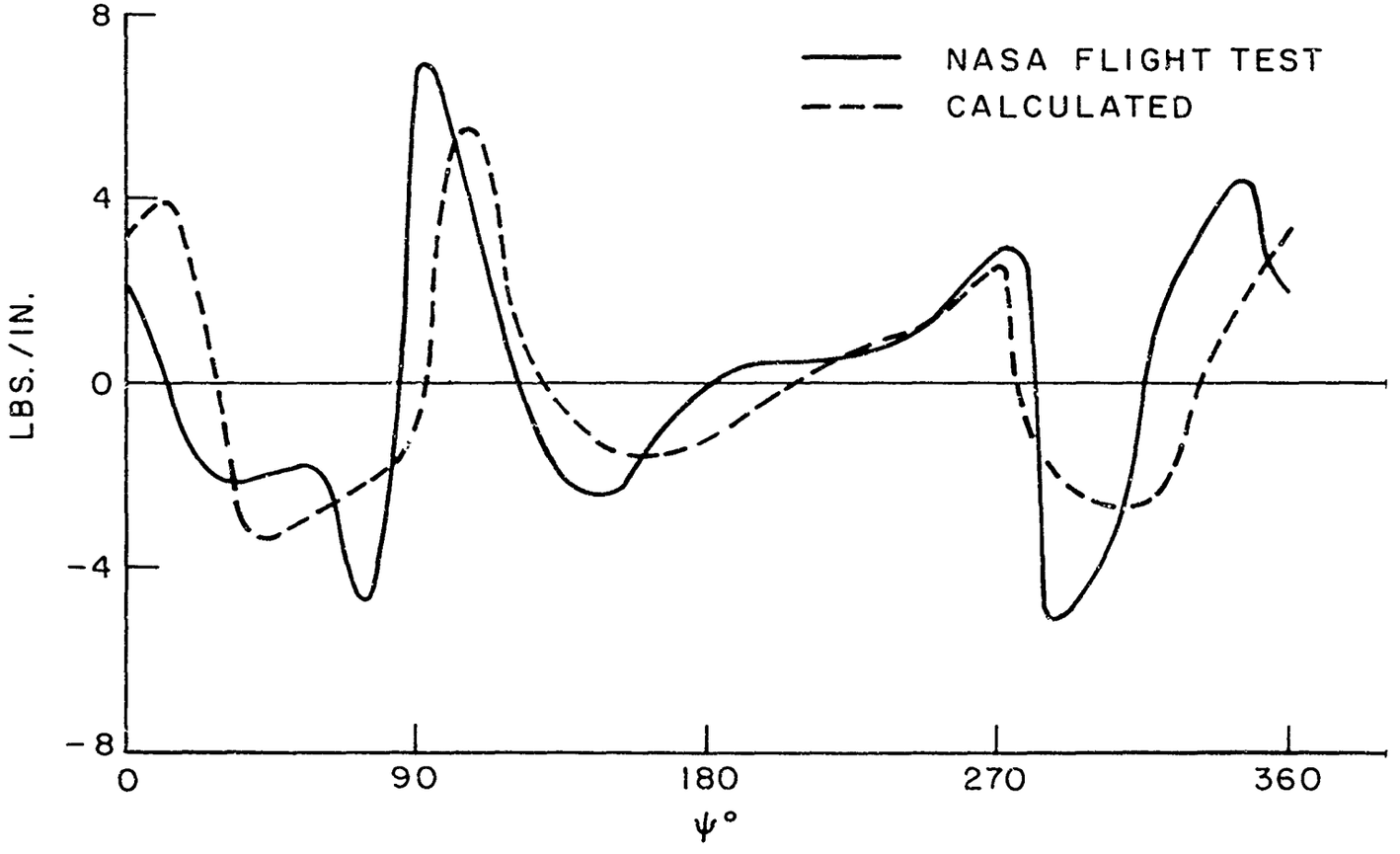

FIG. 6 AIRLOADS, 0th, 1st, AND 2nd HARMONICS EXTRACTED FINITE STRAIGHT LINE 4 BLADES, $\mu = 0.2$, $\lambda = 0.025$, $\eta = 0.95$

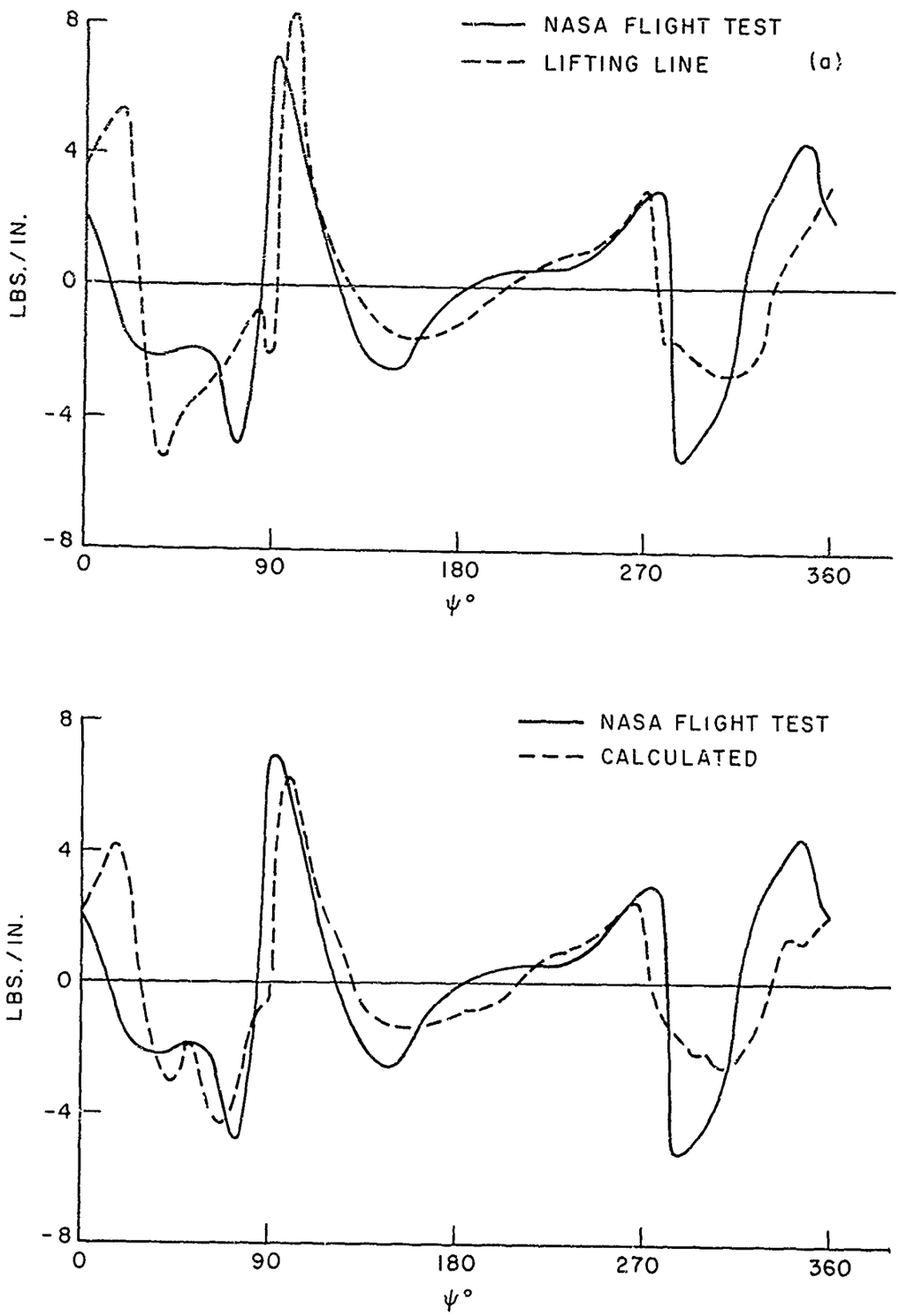

FIG. 7 AIRLOADS, 0^{th}, 1^{st}, AND 2^{nd} HARMONICS EXTRACTED INFINITE STRAIGHT LINE . 4 BLADES, $\mu = 0.2$, $\lambda = 0.025$, $\eta = 0.95$

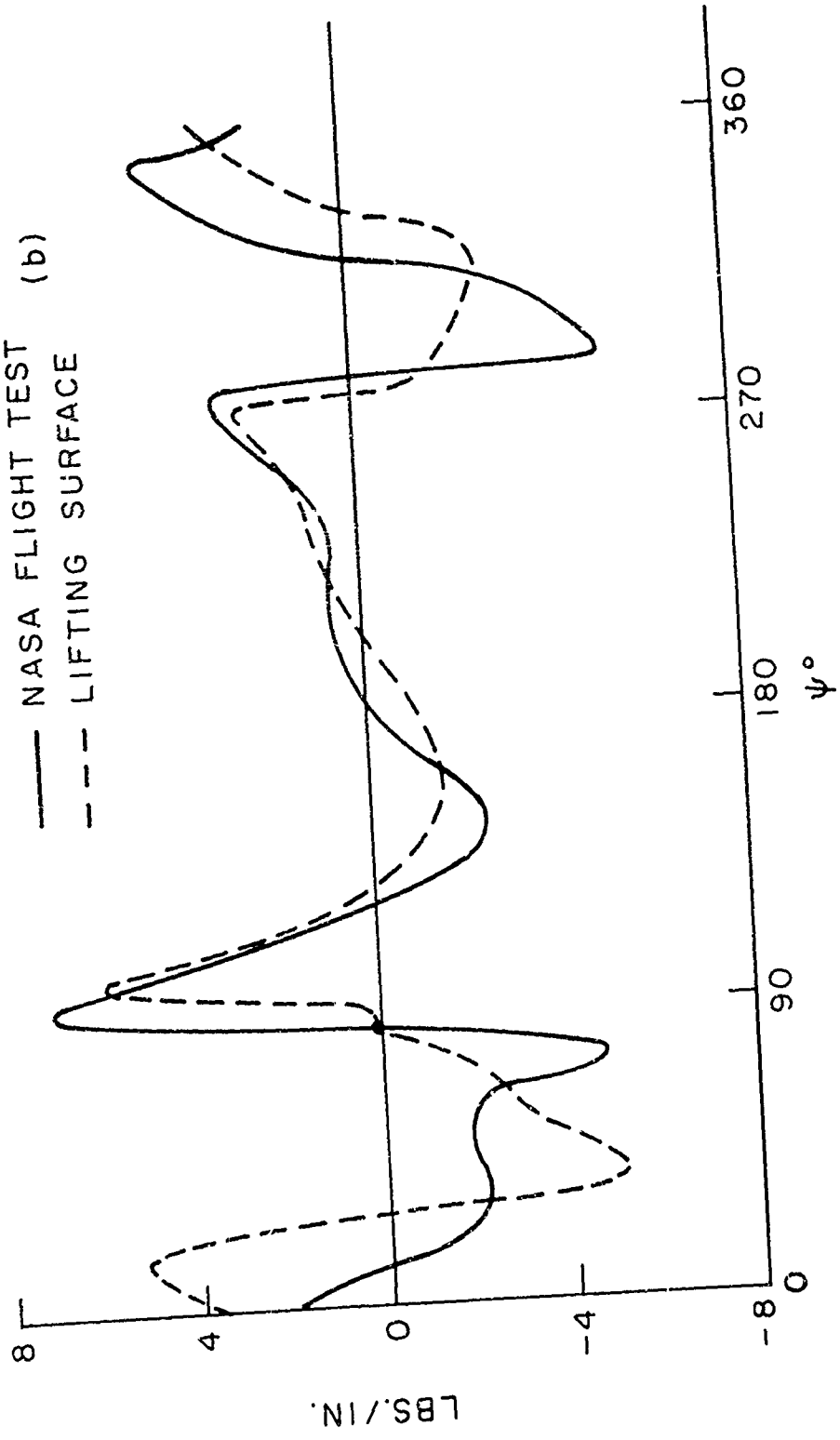

FIG.8 AIRLOADS, 0th, 1st, AND 2nd HARMONICS EXTRACTED, COMPARISON OF TWO DIMENSIONAL LIFTING SURFACE THEORY WITH LIFTING LINE THEORY. 4 BLADES, μ=0.2, η=0.95

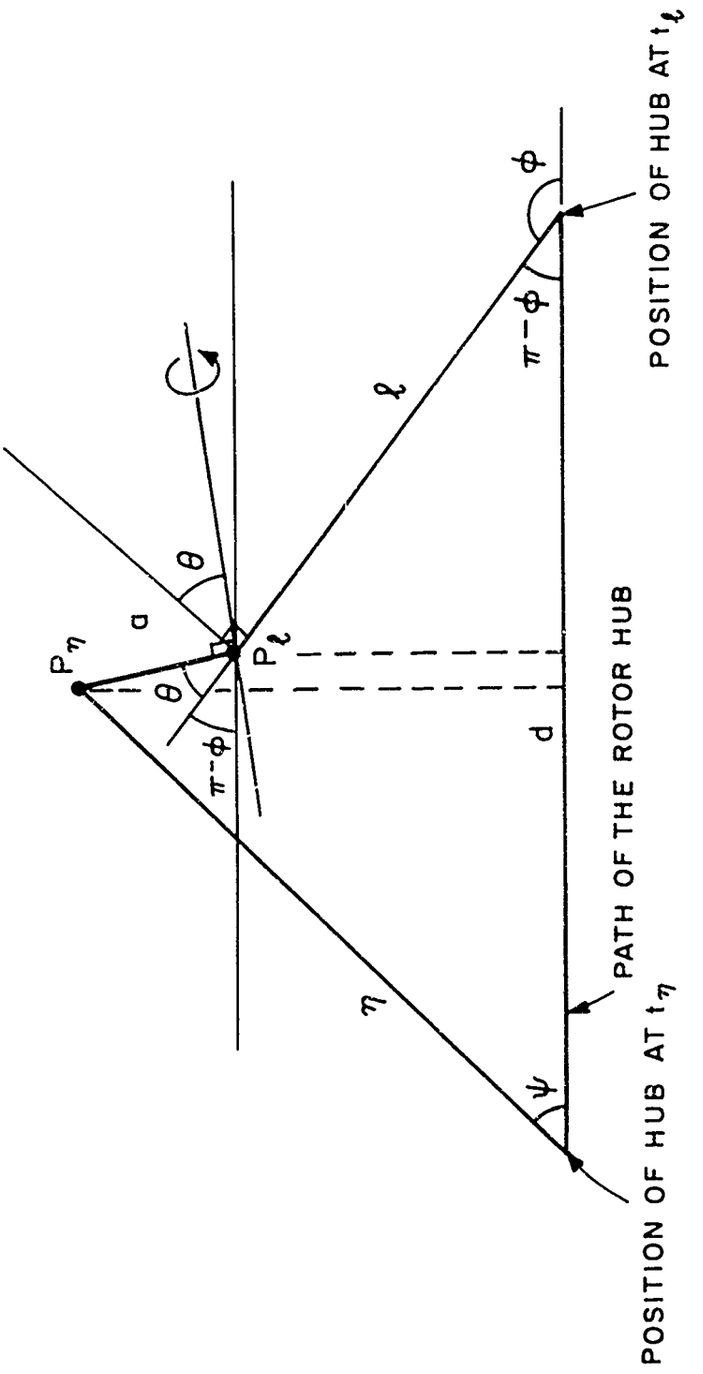

FIG. 9 NEAREST POINT GEOMETRY

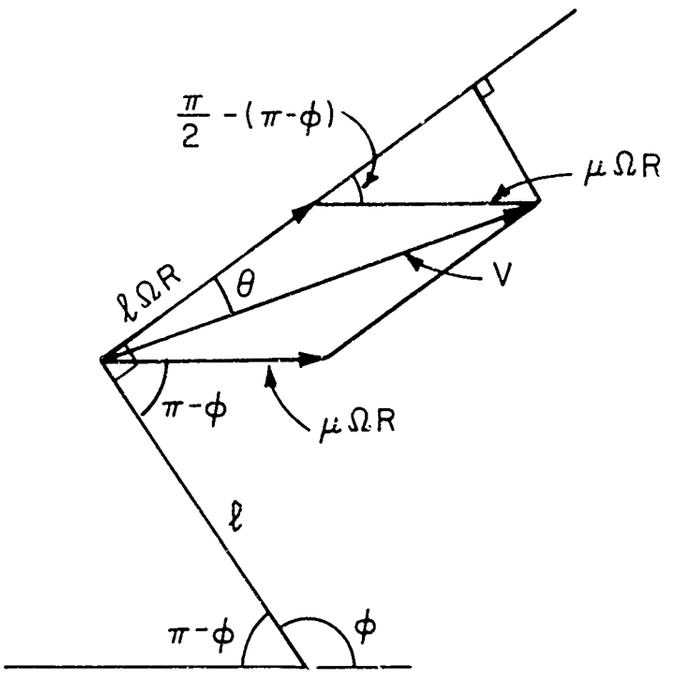

FIG. 10 DERIVATION OF θ

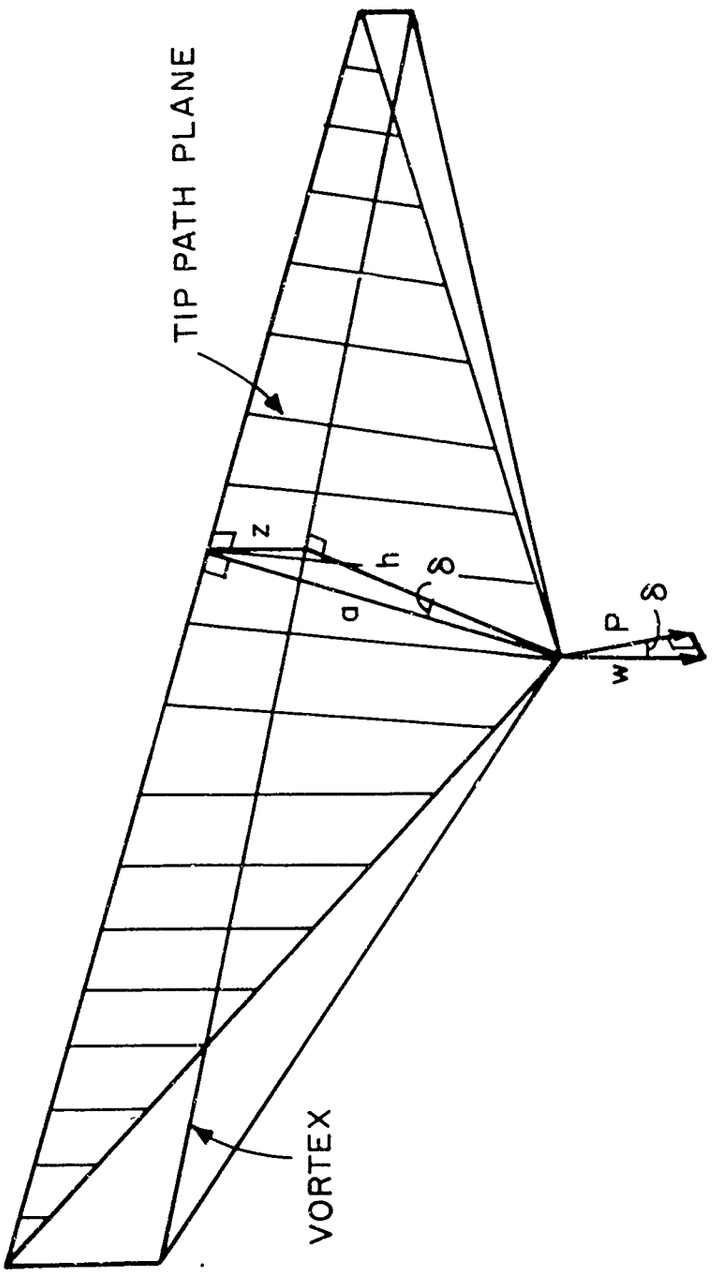

FIG. 11 VORTEX GEOMETRY

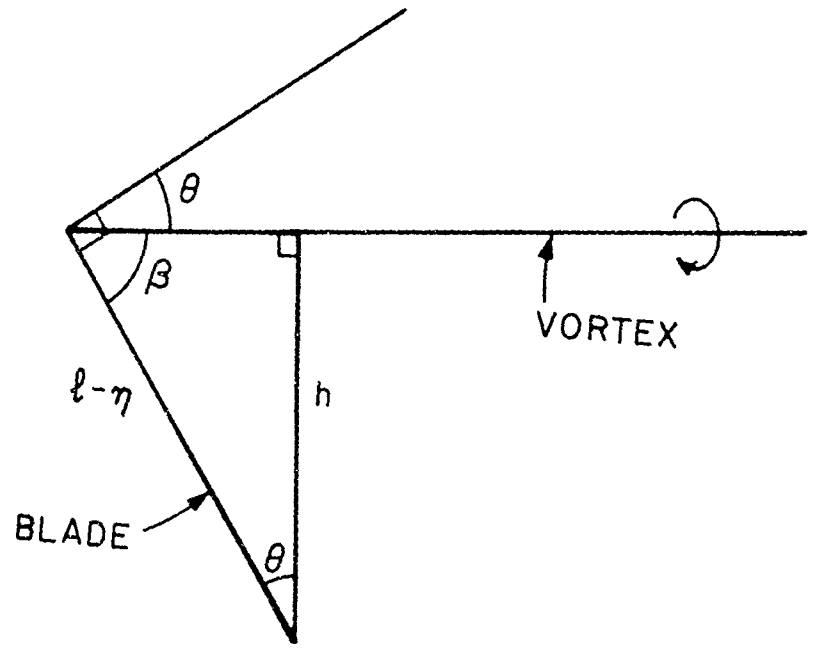

FIG. 12 SINGLE INFINITE VORTEX, NEAR WAKE GEOMETRY

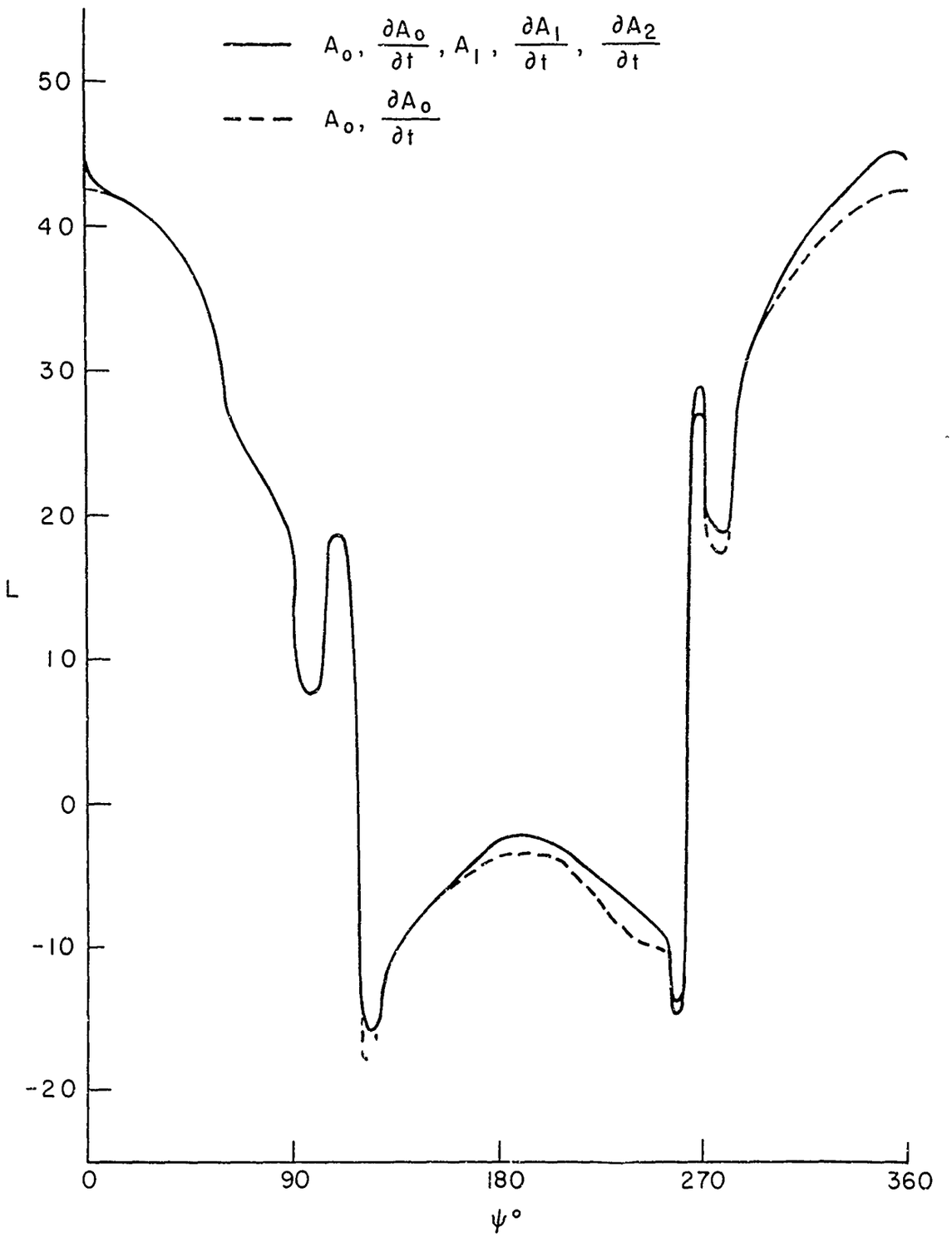

FIG. 13 LIFTING SURFACE APPROXIMATION. 4 BLADES $\mu = 0.2$, $\lambda = 0.025$, $\Delta\phi = 7.5°$, $\eta = 0.85$

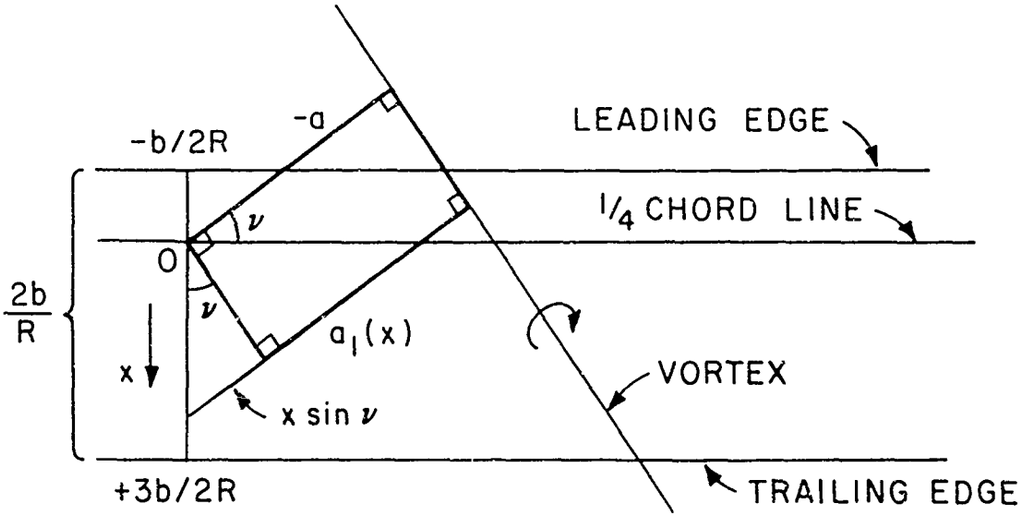

FIG. 14 LIFTING SURFACE GEOMETRY

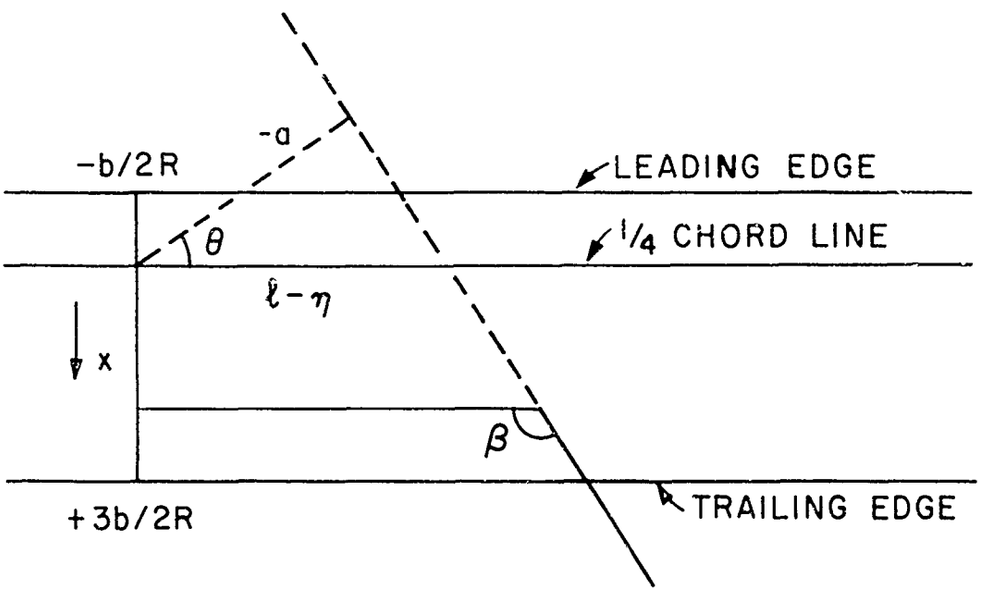

FIG. 15 LIFTING SURFACE, NEAR WAKE GEOMETRY

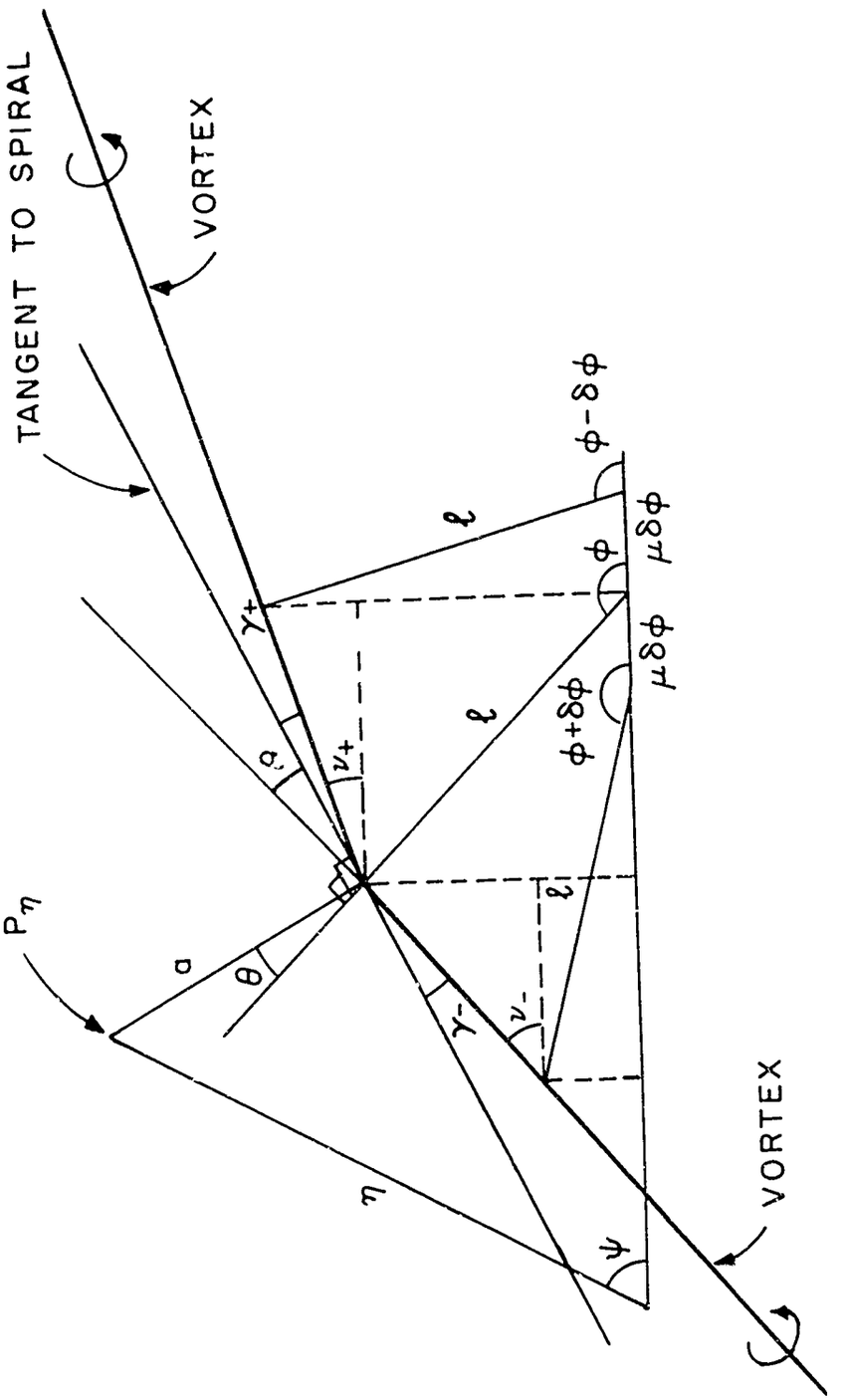

FIG.16 DOUBLE INFINITE VORTEX GEOMETRY

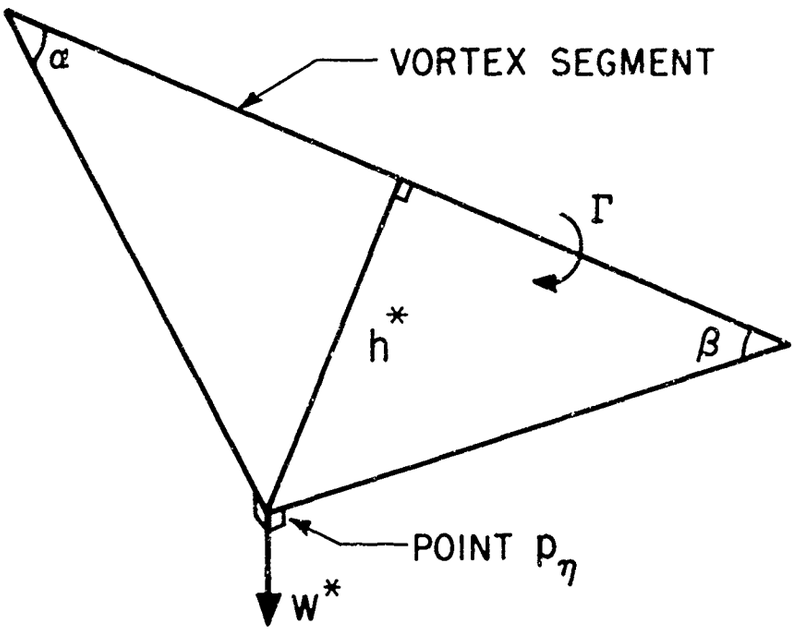

FIG. 17 VORTEX SEGMENT GEOMETRY

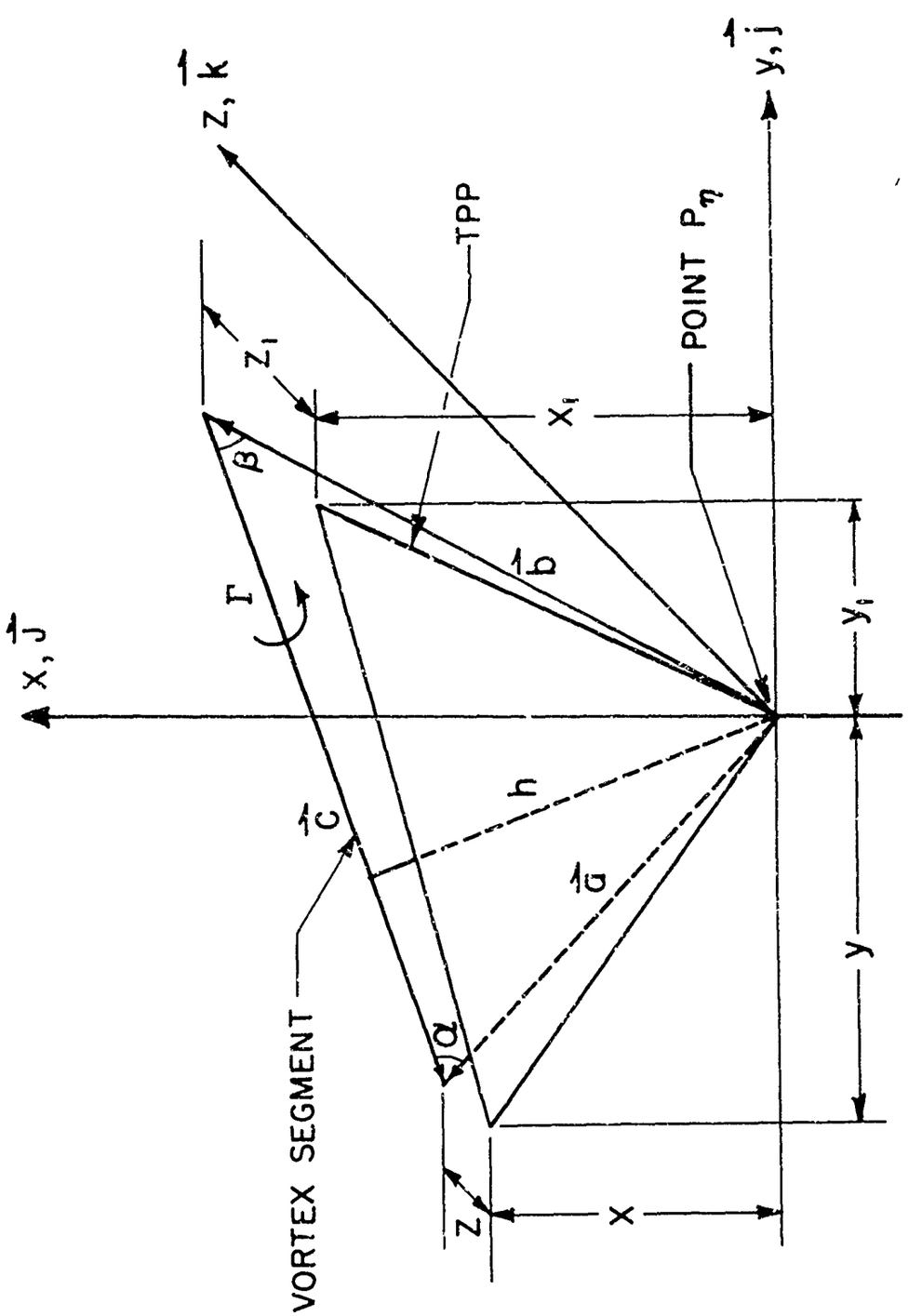

FIG. 18 VORTEX SEGMENT GEOMETRY

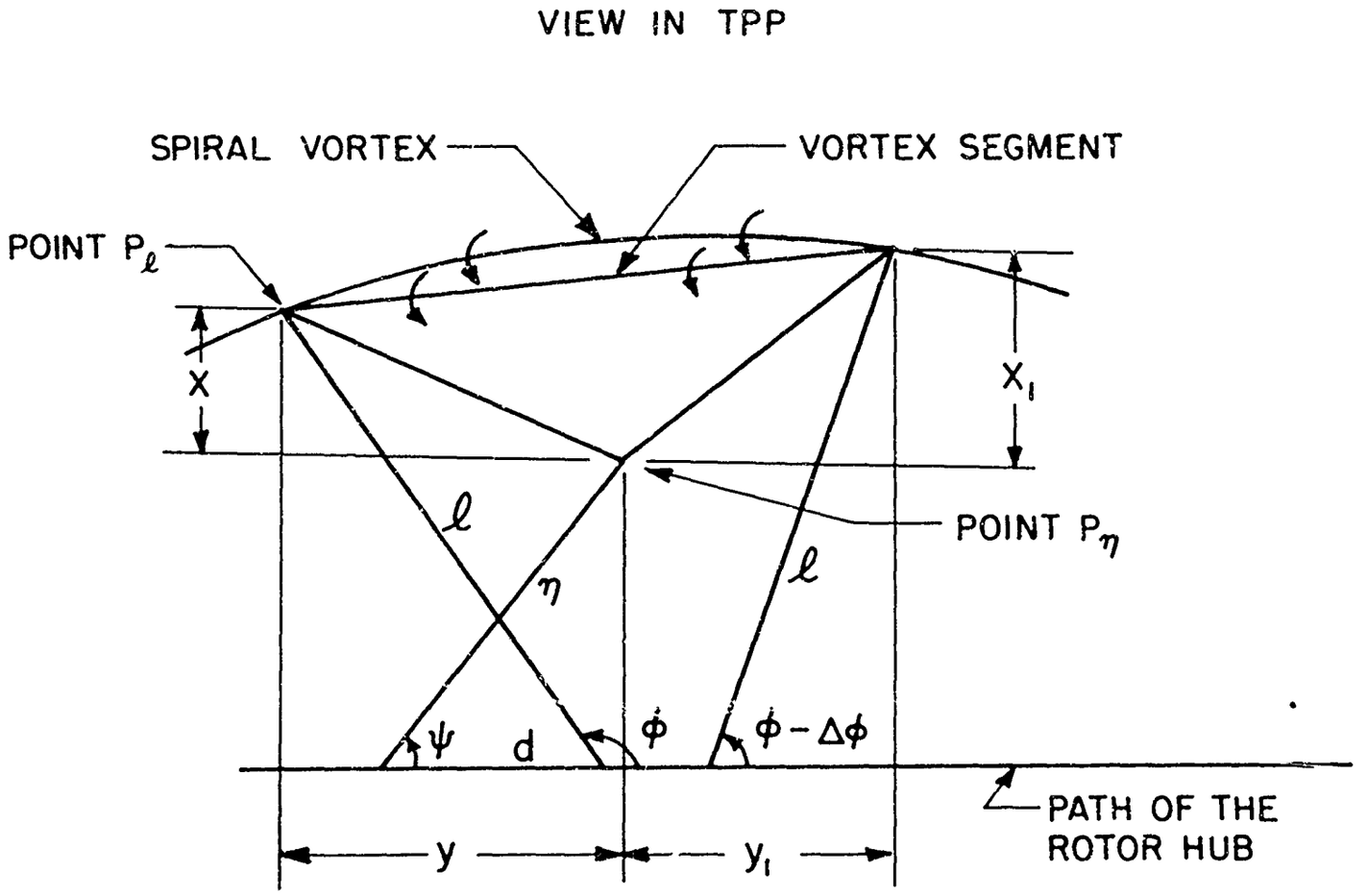

FIG. 19 SPIRAL VORTEX – VORTEX SEGMENT GEOMETRY PROJECTED INTO TPP